Seasonal pattern of influenza and the association withmeteorological factors based on wavelet analysis in Jinan City, Eastern China, 2013 - 2016

Wei Su [Corresp., Equal first author, 1], **Ti Liu** [Equal first author, 2], **Xingyi Geng** [3], **Guoliang Yang** [3]

[1] School of Management Science and Engineering, Shandong University of Finance and Economics, Jinan, Shandong Province, China

[2] Shandong Center for disease control and prevention,, Shandong Provincial Key Laboratory of Infectious Disease Control and Prevention, Shandong University Institution for Prevention Medicine,, Jinan, Shandong Province, China

[3] Jinan Center for disease control and prevention, Jinan, Shandong Province, China

Corresponding Author: Wei Su
Email address: suwei@sdufe.edu.cn

Background: Influenza is a disease under surveillance worldwide with different seasonal patterns in temperate and tropical regions. Previous studies have conducted modeling of influenza seasonality using climate variables. This study aimed to identify potential meteorological factors that are associated with influenza seasonality in Jinan, China.**Methods**: Data from three influenza sentinel hospitals and respective climate factors (average temperature, relatively humidity (RH), absolute humidity (AH), sunshine duration, accumulated rainfall and speed of wind), from 2013 to 2016, were collected. Statistical and wavelet analyses were used to explore the epidemiological characteristics of influenza virus and its potential association with climate factors.**Results**: The dynamic of influenza was characterized by annual cycle, with remarkable winter epidemic peaks from December to February. Spearman's correlation and wavelet coherence analysis illuminated that temperature, AH and atmospheric pressure were main influencing factors. Multiple wavelet coherence analysis showed that temperature and atmospheric pressure might be the main influencing factors of influenza virus A(H3N2) and influenza virus B, whereas temperature and AH might best shape the seasonality of influenza virus A(H1N1)pdm09. During the epidemic season, the prevalence of influenza virus lagged behind the change of temperature by 1-8 weeks and atmospheric pressure by 0.5-3 weeks for different influenza viruses.**Conclusion**: Climate factors were significantly associated with influenza seasonality in Jinan during the influenza epidemic season, and the optional time for influenza vaccination is before November. These finding should be considered in influenza planning of control and prevention.

Seasonal pattern of influenza and the association with meteorological factors based on wavelet analysis in Jinan City, Eastern China, 2013−2016

Wei Su [1*], Ti Liu [2*], XingYiGeng [3*], Guoliang Yang [3]

[1] School of Management Science and Engineering, Shandong University of Finance and Economics, Jinan, Shandong, P.R.China

[2] Shandong Center for Disease Control and Prevention, Shandong Provincial Key Laboratory of Infectious Disease Control and Prevention, Shandong University Institution for Prevention Medicine, Jinan, Shandong, P.R.China

[3] Jinan Center for Disease Control and Prevention, Jinan, Shandong, P.R.China

*These authors contributed equally to this work and should be considered co-first authors.

Corresponding Author:

Wei Su

NO.7366, ErHuan East Road, Jinan, Shandong, 250014, P.R.China

E-mail: suwei@sdufe.edu.cn

Abstract

Background: Influenza is a disease under surveillance worldwide with different seasonal patterns in temperate and tropical regions. Previous studies have conducted modeling of influenza seasonality using climate variables. This study aimed to identify potential meteorological factors that are associated with influenza seasonality in Jinan, China.

Methods: Data from three influenza sentinel hospitals and respective climate factors (average temperature, relatively humidity (RH), absolute humidity (AH), sunshine duration, accumulated rainfall and speed of wind), from 2013 to 2016, were collected. Statistical and wavelet analyses were used to explore the epidemiological characteristics of influenza virus and its potential association with climate factors.

Results: The dynamic of influenza was characterized by annual cycle, with remarkable winter epidemic peaks from December to February. Spearman's correlation and wavelet coherence analysis illuminated that temperature, AH and atmospheric pressure were main influencing factors. Multiple wavelet coherence analysis showed that temperature and atmospheric pressure might be the main influencing factors of influenza virus A(H3N2) and influenza virus B, whereas temperature and AH might best shape the seasonality of influenza virus A(H1N1)pdm09. During the epidemic season, the prevalence of influenza virus lagged behind the change of temperature by 1-8 weeks and atmospheric pressure by 0.5-3 weeks for different influenza viruses.

Conclusion: Climate factors were significantly associated with influenza seasonality in Jinan during the influenza epidemic season, and the optional time for influenza vaccination is before

November. These finding should be considered in influenza planning of control and prevention.

Key words: Influenza surveillance; wavelet analysis; seasonality; climate factors

Introduction

Influenza remains a global public health concern, causing 3-5 million severe illnesses and 291-646 thousand deaths (Iuliano et al., 2018). Influenza epidemics show distinct seasonality pattern, particularly in winter in temperate areas and a more diverse behavior in tropical and subtropical areas, where influenza displays semi-annual or annual epidemic cycles, and year-round activity (Tamerius et al., 2013). Moreover, the durations and transmission of influenza outbreaks vary among periods (Onozuka et al., 2015). Azziz Baumgartner et al (2012) showed that 7 of 47 (15%) temperate countries presented two or three influenza epidemic period every year, and year-round activity in 3 of 43 (7%) temperate countries. Thus, accurately documenting the dynamics of influenza epidemics and understanding its epidemic patterns are of great importance not only to scientific interest, but also public health (Thai PQ et al., 2015).

The seasonality of influenza epidemics is associated with many factors, including virus mutation, people susceptibility, climate, and environmental changes. Among all of the factors, climate plays the most important role in influenza seasonality (Lofgren et al., 2007; Lowen et al., 2014; Tamerius et al., 2011). Experimental studies in guinea pigs showed that the influenza is stable at low relative humidity (RH) and relatively unstable at intermediate RH, with absolute humidity (AH) impacting the influenza virus viability and transmission. Yang et al. (2012) proposed that the effect of RH on influenza stability may be due to changes in salt concentration within droplets. Influenza virus is also more stable at low temperatures, which may be due to an increased virus half-life at low temperatures, decreased activities of proteases, and cooler epithelial surface (Aniceet et al. 2014). Furthermore, temperature and RH influence the innate

defense of host nasal epithelia and the production of infectious bio-aerosols, thereby shaping influenza seasonality. Some studies have hypothesized that influenza virus stability increases with reduced sun activity (Hope-Simpson, 1981).

To evaluate whether climate factors shape the seasonality of influenza, epidemiological studies comparing influenza seasonality to metrological conditions have been performed, showing that lower temperature and AH increase influenza virus survival and transmission in temperate regions (Shaman et al., 2009, 2010, 2011). Tamerius et al. (2013) and Bloom-Feshbach et al. (2013) showed that the onset of influenza epidemics is associated with the cold-dry and humid-rainy condition in temperate and tropical areas, respectively. After analyzing the relative reports of 11 locations in different climate regions, K.C. Chong et al (2019) found that temperature and AH were the major determinant to influenza A and influenza B, and RH was less consistent with influenza B activity. While Peci A et al (2019) reported the negative relationship of both AH and temperature with influenza virus A and B and a controversial effect of RH on influenza virus A and B. Although influenza patterns have been well described in developed temperate regions, those involving developing temperate areas are limited. Yu et al. (2013) showed that minimum temperature, the hours of sunshine and maximum rainfall are closely related with influenza seasonality in China, but AH was not taken into consideration, and the influenza surveillance data from April-September in northern China was missing. Several studies teams demonstrated the negative association between influenza virus with temperature and AH in Beijing and Gansu Province, North of China, respectively (Chao et al., 2010; Sun et al., 2018; Yang et al., 2019). However, studies on the relationship between different influenza virus types or subtypes and

climate factors are limited. Therefore, understanding the influence of climate factors is vitally important to learn the influenza seasonality pattern and consequently implement prevention and control strategies.

In this study, we analyzed the seasonality of influenza and explored various climate factors, including AH, RH, temperature, atmosphere, the hours of sunshine, wind speed, and accumulated rainfall as potential drivers to the seasonality of laboratory-confirmed influenza cases in Jinan City, the capital of Shandong Province, eastern of China, from 2013 to 2016. Jinan is a temperate city with 7 million people and 3 sentinel hospitals for the surveillance of influenza. This detailed analysis of influenza pattern aim to provide evidence to foster strategies to prevent and control influenza in future years.

Methods

Influenza surveillance data

Epidemiological and virology data of three national influenza surveillance sentinel hospitals was collected from Jinan Center for Disease Control and Prevention for the study period of 2013–2016, including QiLu Children's Hospital of Shandong University, the No. 4 Hospital of Jinan, and the No. 6 Hospital of Jinan (The People's Hospital of Zhang-QiuArea, Jinan) located in different 3 zones and represented about a third of the total population. For each hospital, at least 20 nasopharyngeal swab specimens were collected each week from patients with influenza-like illness (ILI), which was defined as an outpatient of any age with an acute respiratory infection syndrome with fever ≥38°C and cough or sore throat. All collected samples were tested for influenza virus by virus isolation in Madin-Darby canine kidney cells. The types (influenza A

and B), subtypes (A(H3N2) and A(H1N1)pdm09), and lineages of influenza B (Yamagata and Victoria) were identified by haemagglutination assay and haemagglutination inhibition (HI) test according to National Influenza Surveillance Protocol published by Chinese Health commission of the People's Republic of China. In this study, we used the weekly positive rate of different influenza virus types or subtypes as influenza proxy (Positive rate = Number of positive specimens/Total number of specimens tested per week ×100%) to describe the seasonality of influenza according to Tameriu et al. (2011) and Liu et al. (2017).

Climate data

Weekly meteorological data from 2013 to 2016 from Jinan were obtained from Meteorological Science Data Sharing Service System, including weekly average values of temperature (°C), atmospheric pressure (hPa), RH (%), wind speed (m/s), accumulated rainfall (mm), and sunshine duration (h). The weekly average AH (g/m^3) was calculated based on the data of average temperature and RH using the formula described by Xiao et al. (2012).

Statistical methods

A descriptive analysis was used to reveal the characteristics of influenza epidemics and climate factors. To characterize the epidemics of influenza, continuous wavelet transform (CWT) was applied to uncover the time frequencies of influenza virus (Cazelles et al. (2007). This technique has been widely used to explore the temporal and spatial variations of different infectious diseases, including influenza (Xiao et al., 2012; Liu et al., 2017). Wavelet transform can divide the time series into a family of wavelets using dilated and translated functions called "mother wavelets". In this study, the Morlet wavelet was selected as the mother, which can be well

localized in scales and in high-frequency resolution and is regarded as an efficient means of detecting and analyzing the time series (Ng et al. 2012). Wavelet analysis is represented by a colored contour. The 5% significant level against red noise is shown as a thick black curve. The cone of influence, which indicates the region affected by edge effects, is shown with a lighter shade. The color code for power ranges from pink (low power) to white (high power).

To explore the potential relationship between influenza and climate variables, Spearman's correlation was conducted to determine the correlation between different climate factors and influenza virus types or subtypes.

Wavelet transform coherence (WTC) was used to investigate the possible inter-connectedness between influenza and climate variables according to the method described by Grinsted et al. (2004). The WTC shows the significant coherence against red noise in time-frequency space, which can depict the significant covariance at specific periods (frequencies) and phase shift between two time-series. The phase difference between the two series is indicated by arrows. If the arrow points to the right (left), the series are positively (negatively) correlated, i.e., they are in the in-phase or the anti-phase, respectively, and if the arrow points straight down (up), the first series leads the other by 90° (vice versa). For the detail information, please refer to the method described by Grinsted et al. (2004).

Finally, to exploit the possible relationship between influenza and climate factors, multiple wavelet coherence (MWC) was applied. MWC is a technique that is similar to multiple correlations and helps to seek the resulting wavelet coherence of two independent variables on a dependent one at a given time and frequencies (Grinsted et al. 2004; Ng and Chan 2012).The

150 continuous wavelet analysis, wavelet transform coherence and MWC were performed based on a
151 library of MATLAB functions provided by Grinsted et al. (2004)
152 (http://noc.ac.uk/business/marine-data-products/cross-wavelet-wavelet-coherence-toolbox-
153 matlab).

154 **Results**

155 **Descriptive statistics**

156 **Seasonality and periodicity of influenza virus in Jinan**

157 A total of 9170 ILI samples were collected, and 914 laboratory-confirmed cases (9.94%) were
158 identified by virus isolation from 2013 to 2016, including 370 influenza virus A(H1N1)pdm09,
159 299 influenza virus A(H3N2), and 245 influenza virus B (219B/Yamagata lineage and 26
160 B/Victoria lineage) (Table 1). A(H1N1)pdm09 and A(H3N2) were detected from 2013 to 2016,
161 accounting for 73.19% of the total positive influenza virus cases. Figure 1A shows the seasonal
162 distribution of different influenza types, subtypes and lineages during the periods, which clearly
163 indicated that influenza had seasonality, with one epidemic peak during the winter season. Figure
164 1B revealed the wavelet power spectrum of the influenza virus. A high-power spectrum indicated
165 dominant frequency- and time-specific periodicity. Although annual influenza epidemic cycles
166 were identified in the 32–64 week band (2013–2016) with high power, influenza virus also
167 showed a distinct epidemic peak with high power in the 8–14- and 0–4-week bands in 2014–
168 2015 and 2014–2016 ($p<0.05$), respectively.

169 Figure 2 demonstrates the seasonality of influenza virus A and B in Jinan. Similar to the total
170 influenza activity, A(H3N2)、A（H1N1）pdm09 and influenza virus B showed an annual

171 cycle with a peak in winter (Figure 2A, 2C and 2E). Based on CWT, A(H3N2) exhibit a
172 statistically significant periodicity during 2014-2015 with higher power in the 0-4 week band
173 (Figure 2B), and A(H1N1)pdm09 had two statistically significant regions in 2015-2016 with
174 higher power in the 0-4 and 8-16 week bands (Figure 2D). Influenza virus B exhibited a
175 statistically significant periodicity with three regions of high powers in the 0-4 week band during
176 2014-2016 and one high power in the 6-24 week band in 2014-2015 (Figure 2F).

177 **Seasonality and periodicity of climate factor in Jinan**

178 Table 1 showed the average values of the weekly climate factors: atmospheric pressure,
179 temperature, and RH, AH, wind speed, sunshine duration, and accumulated rainfall during the
180 study period. Figure 3 demonstrates the weekly variation in climate factors with clear seasonal
181 and periodic characteristics. Atmospheric pressure and influenza positive rate showed similar
182 patterns, but average temperature and AH exhibited different variations.

183 **Spearman's correlation**

184 Table 2 shows the relative spearman's correlation of different influenza viruses and climate
185 factors. Spearman's correlation analysis shows that weekly average atmospheric pressure is
186 positively correlated with influenza. In contrast, weekly average values of temperature, AH, RH,
187 and accumulated rainfall are negatively associated with influenza. The spearman's correlation
188 between climate factors and three influenza virus types or subtypes demonstrated medium
189 association for atmospheric pressure, temperature and AH and weak relationship for RH and
190 accumulated rainfall. Influenza has no correlation with the weekly average wind speed and the
191 weekly average sunshine duration ($p > 0.05$), except for A(H3N2) with the weekly average wind

192 speed. Based on these observations, atmospheric pressure, temperature, AH, RH, accumulated
193 rainfall, and wind speed (only for A(H3N2)) were selected for further analysis.

194 **Wavelet transform coherence (WTC)**

195 The results of WTC of influenza and different climate factors are shown in Figures 4–6. WTC
196 provided information on whether two time series are linearly correlated or co-moved at a
197 particular time and frequency, in which the whiter the color, the higher the correlation.
198 Statistically significant relationships are highlighted by a thick black curve around the significant
199 regions. The cone of influence is shown with a lighter shade black line. The color code for power
200 ranges from pink (low power) to white (high power). The orientation of the arrows represents the
201 lag or lead relationship. The down arrows show climate factor is leading. The up arrows denote
202 influenza is leading.

203 For influenza virus A (H3N2), the result of WTC shows that it is statistically significantly
204 associated with some climate factors in some periods (Figure 4). The atmospheric pressure was
205 significantly correlated at the period of approximately 26 week band (2013–2014) ($p<0.05$),
206 with arrows pointing to the left, indicating that both are negatively correlated during 2013–2014.
207 For temperature, A(H3N2) was significantly correlated at the period of approximately 26 week
208 band (2013–2014), and the arrows pointed down, indicating that the changes of temperature
209 leads the prevalence of influenza by 8 weeks. For RH, we also observed one high-power
210 spectrum in the 8–12 week band (2014–2015) with anti-phase, indicating that both are negatively
211 correlated during the period. At the same time, in the 32–64 week timescale, we found a strong,
212 but not statistically significant at the 5% level, correlation during the study period between

A(H3N2) and different climate factors, showing that atmospheric pressure is positively correlated and the other climate factors except for wind speed were negatively correlated with A(H3N2) on the annual cycle during the periods.

For influenza virus A(H1N1)pdm09, we also observed a statistically significant association with atmospheric pressure, temperature, RH, and AH on the short or medium scales (Figure 5). For atmospheric pressure, A(H1N1)pdm09 was significantly negatively correlated at periods of approximately 26 week band (2014) and 1–12 week band (2014–2015). The power was also observed in the 3–6 week band in 2013-2014 with arrows pointing down, which illuminated that the prevalence of influenza virus lags by approximately 0.5-1 week. In terms of temperature, in the 26 week band (2013–2014), A (H1N1) pdm09 was negatively correlated. For the periods of 6–10 week band in 2015–2016, we observed a negative relationship, in which the change of temperature leads the prevalence of influenza virus by approximately 2–3 weeks. But for the bands of the 6–8- (2013–2014) and 6–12- (2014–2015) week, positive correlations were observed. At the same time, a significant period of 4–6 week band (2015–2016) of AH were also observed, showing that the change of AH leads the prevalence of influenza virus by 2–3 weeks during the periods. For RH, we only observed a statistically significant region in the 8–10 week band (2014–2015), with influenza virus leading. Similar to A (H3N2), on the one-year scale, atmospheric pressure was positive and the other climate factors except for rainfall were negative with A(H1N1)pdm09 during the periods.

For influenza virus B, we observed statistically significant correlation with atmospheric pressure in the approximately 26 week band (2014-2015) and 6–10 week band (2015–2016) (Figure 6A),

234 with the change of atmospheric pressure leading the prevalence of influenza by 3 weeks and 1–
235 1.5 weeks, respectively. For temperature, influenza virus B was significantly correlated at
236 periods of approximately 6-12 week band (2013-2014), showing that temperature leads influenza
237 by 1-2 weeks. Similarly, atmospheric pressure was positively correlated and the other climate
238 factors were negatively correlated with influenza virus B on the one-year scale (Figure 6).

239 **Multiple wavelet coherence analysis**

240 After WTC, temperature, humidity (AH and RH), and atmospheric pressure were involved with
241 MWC analysis. The combined impact of any two of four different climate factors and influenza
242 virus can be analyzed using MWC squared. The plots of MWC of three influenza virus types or
243 subtypes are shown in Figures 7–9. Through MWC by comparing different combinations of the
244 climate factors, the results show that not only the short-term (8–14 week band), but also the
245 medium-term (26 week band) and the long-term trend relationships or co-movement between
246 climate factors and influenza virus types or subtypes are correlated. For example, the MWC
247 (influenza A(H3N2)-temperature-RH) plot in Figure 7C shows that three time series are
248 correlated significantly and share the same coherent areas in the 26 week band (2013–2016) and
249 in the 6–12 week period (2013–2016). Thus, based on figures 7–9, we concluded that the
250 combination of temperature and atmospheric pressure, temperature and AH, and temperature and
251 atmospheric pressure were the main potential influencing factors of influenza virus B,
252 A(H1N1)pdm09, and A(H3N2), respectively.

253 **Discussion**

254 In this study, we exploited influenza seasonality and the potential relationship between influenza

seasonality and different climate factors. Through descriptive analysis and wavelet analysis, we found that influenza virus exhibited an annual epidemic cycle with remarkable winter seasonality in Jinan, and concluded that the potential relationships or co-movement of influenza virus types or subtypes and different climate factors were quite correlated in Jinan from 2013 to 2016.

The laboratory-confirmed data is thought to be a better indicator to depict the influenza seasonality (Tamerius et al., 2011; Liu et al., 2017), compared with influenza-like illness which was used to represent the level of influenza activity in some studies (Azziz et al., 2012; Thai et al., 2015; Tamerius et al., 2011). Thus, in our study, the weekly positive rate of influenza virus was used to precisely illustrate the epidemic and seasonality of influenza. The description statistics and CWT analysis indicated that influenza had an annual cycle with regular peak seasonality in winter season and was scarce in the summer and autumn seasons in Jinan City, which was in accordance with the findings of previous reports in temperate regions (Wu et al., 2016; Caini et al., 2016, 2017). The CWT analysis further illuminated that the onset of epidemic of influenza always began in December and the epidemic peak time could last for 8–14 weeks in every surveillance year (Figure 1B). Unlike other studies in which influenza had two or three peaks in a temperate zone (Azziz et al., 2012), we only found an obvious epidemic peak in Jinan. By analyzing the time series of each influenza virus type or subtype, the descriptive analysis and CWT analysis also showed that three influenza viruses were detected every year with one or two subtypes predominated in winter, and the predominant subtype changed with the years. In the early stage of 2013, A(H1N1)pdm09 was the main epidemic virus. In 2013–2015 surveillance years, influenza virus B and A(H3N2) were the main epidemic strains with few A(H1N1)pdm09

276 detected. In 2015–2016 surveillance year, the predominant virus was changed to
277 A(H1N1)pdm09 and A(H3N2) become the predominant virus in the last month of 2016.
278 Therefore, understanding the influenza seasonality suggested that the optional time of influenza
279 vaccination programs was from September to November in Jinan, which provided immune
280 protection in the epidemic peak time. Otherwise, the vaccine effectiveness wanes over time
281 (Kissling et al., et al., 2013; Ebody et al., 2013).
282 The seasonality of influenza indicated a peak in winter and the predominant influenza virus
283 changed with the years. As for the mechanism of the seasonality and alternation of influenza,
284 host susceptibility, virus mutation, and climate factors may have driven influenza virus
285 circulation activity. Therefore, we exploited the potential association between influenza virus
286 subtypes and different climate variables through the WTC analysis and MWC analysis. We
287 speculated weekly change in climate variables significantly contributed to dynamic variation of
288 influenza, which was in agreement with the findings of previous studies (Tamerius et al., 2013;
289 Onozuka et al., 2015; Azziz et al., 2012; K.C. Chong et al., 2019). Through WTC analysis and
290 MWC, we concluded that there were statistically significant associations between atmospheric
291 pressure, temperature, and humidity (RH and AH), and influenza seasonality.
292 For weekly atmospheric pressure, we observed that there was positive association with three
293 different influenza virus subtypes in the annual cycle, but this relationship varied with week time
294 scales during 2013–2016, which was consistent with the findings of previous studies in avian
295 influenza viruses (Li et al., 2015; Soebiyanto et al., 2010). On the short- and the medium-term,
296 atmospheric pressure may influence the variations in different influenza virus types, which

297 concluded that atmospheric pressure may be a driver of influenza. The results were verified by
298 MWC analysis, which was consistent with the results of Sundell et al. (2016). Furthermore,
299 during some time periods, the prevalence of influenza virus lags the changes in atmospheric
300 pressure, which may speculate the occurrence of A(H3N2) epidemics. The reason could be that
301 the mucous membrane of nasal cavity was easily broken in dry conditions and high atmospheric
302 pressure in the winter season, and virus could easily infect it. However, the detailed mechanism
303 requires further investigation.
304 Temperature was often reported to be associated with influenza seasonality, especially in warm
305 regions with influenza epidemic peaking in the winter (Yu et al., 2013; Soebiyanto et al., 2010;
306 Tamerius et al., 2019). In Jinan, we also observed a negative association between average
307 temperature and three influenza virus subtypes through spearman's correlation analysis and
308 WTC. Except for the negative relationships, we also observed that during some time periods,
309 changes in temperature lead the prevalence of A(H1N1)pdm09 and influenza virus B by 2–3
310 weeks (2015–2016) and 1-2 weeks (2013–2014), respectively. Therefore, temperature may be
311 a good predictor of influenza virus epidemics, not only influenza virus A, but also influenza
312 virus B, which was consistent with the results of K.C. Chong et al (2019) and Peci A et al (2019).
313 Indeed, most of the studies demonstrated that temperature was a dominant determinant of
314 influenza virus A and B in temperate regions, which was observed in a guinea pig model (Low
315 AC et al. 2014). Several studies showed that influenza is more stable at low temperature which
316 decreases activities of proteases, reduces the mucus and ciliary movement and inhibits defense
317 and immunity toward infection, thus affects the host susceptibility and increases the transmission

of influenza virus in winter (Aniceet et al. 2014; Peci A et al. 2019). Lowens et al. (2014) further verified that the influenza transmission was most efficient at low temperature (5℃), the transmission and survival capacity declined as temperature increased from 5℃ to 20℃ and was completely blocked at 30℃ based on the study conducted in guinea pigs. In Jinan, the influenza peak always occurred in December–February with mean temperature at -5°C to 5°C, which increased the influenza transmission.

For RH, we observed the weakly negative association with three influenza virus subtypes with spearman's correlation analysis and WTC in different week bands during various periods, and we did not observe any lead correlations with influenza. Similarly, Noti et al. (2013) found that influenza virus remains five times more infectious at low RH (7-23%) than at an RH of 43% and above. The mechanism would be explained that the virus aerosol remains a longer time at low RH and increased the opportunity to infect new hosts (Sundell N et al. 2016)

In the study, we also observed a negative association between AH and influenza virus. For A(H1N1)pdm09, change in AH leads the prevalence by 2–3 weeks during 2015–2016, which revealed that AH may be a good predictor of A(H1N1)pdm09. For influenza B, we also observed a potential negative correlation during the 8–12 week band during 2013–2014. MWC analysis further demonstrated that AH might influence the seasonality of influenza virus, which coincided with the experimental results in guinea pig and the epidemiology data analysis (Lowen et al. 2007; Shaman et al., 2007, 2010, 2011; Lowen et al., 2014).The mechanism may be that the high level of AH deactivate the virus surface because of the denaturing of virus lipoproteins (Yang W. et al.2012)

Previous studies have reported that the amount of rainfall increases influenza virus activity in tropical and subtropical areas such as Thailand, Guiana in French (Pica et al., 2012; Mahamat et al., 2013). However, in our study, we observed a poor relationship between the accumulated rainfall with A(H3N2) and influenza virus B on one-year scales, which is consistent with the findings in Egypt in which the infection of H5N1 avian influenza was negatively associated with precipitation between 2006 and 2008 (Monamele et al., 2017; Murray et al., 2011). In Jinan, the rainfall season is mainly concentrated in summer with the average temperature >30℃, and dramatically decreases the half-time of influenza virus and transmission capacity. However, we did not observe a relationship between influenza virus and the sunshine duration in our study, which is different from the study of Yu et al. (2013), in which sunshine duration is a key environmental variable in influenza virus transmission.

MWC analysis indicated that the combination of any two of four climate factors influenced the seasonality of different influenza virus types or subtypes. Temperature and atmospheric pressure might be the main influencing factors of A(H3N2) and influenza virus B, whereas temperature and AH might best shape the seasonality of A(H1N1)pdm09. Therefore, we conclude that the influenza seasonality may be influenced by some of the relative climate factors, not by one single climate factor (Tamerius et al. 2011). In 2014–2015 influenza epidemic seasons, atmospheric pressure, temperature, and RH influenced the seasonality of A(H3N2) and A(H1N1) pdm09; whereas atmospheric pressure, temperature, AH, and RH influenced the seasonality of influenza virus B and A(H1N1)pdm09 in the 2015–2016 influenza epidemic seasons.

The study had some interesting findings. First, the dynamic variation of influenza was clear with

a peak time in winter season in Jinan, which provided the scientific support for further measure to prevent and control influenza virus, including vaccination time, the time of taking measure by health committee and the high-risk populations.

Second, atmospheric pressure may influence the activity of influenza virus. Previous studies seldom focused on the effect of atmospheric pressure on influenza. In our study, we concluded that atmospheric pressure was positively correlated with three influenza virus types or subtypes, which was used for the influenza virus prediction in the future analysis.

Third, different combination of climate factors may influence different influenza viruses, which further predict the seasonality of different influenza viruses. Spearman's correlation analysis and WTC demonstrated that temperature, AH and atmospheric pressure were main influencing factors, and the strength of different combination of climate factors contributed to the seasonality of different influenza virus, which provided a new idea for influenza prevention and control.

Conclusions

In all, based on the wavelet analysis, we found the dynamic variations in influenza virus characterized by annual cycle with remarkable winter seasonality and exploited the potential impacts of climate parameters on influenza virus: temperature and atmospheric pressure might be the main influencing factors of A(H3N2) and influenza virus B, whereas temperature and AH might best shape the seasonality of A(H1N1)pdm09. Wavelet analysis indicated that changes in different climate factors lead to different extents of delays in influenza virus occurrence. All of this provides scientific support for influenza virus prevention and control.

Acknowledgments

We are grateful to the staff of the influenza surveillance sentinel hospitals.

References

1. Azziz Baumgartner E, Dao CN, Nasreen S, Bhuiyan MU, Mah-E-Muneer S, Al Mamun A, Sharker MA, Zaman RU, Cheng PY, Klimov AI, Widdowson MA, Uyeki TM, Luby SP, Mounts A, Bresee J.. 2012.Seasonality, timing, and climate drivers of influenza activity worldwide. *J Infect Dis*. 206(6):838-46. doi: 10.1093/infdis/jis467.

2. Anice C. Lowen John Steel. 2014. Roles of humidity and temperature in shaping influenza seasonality. Journal of virology7692-7695

3. Bloom-Feshbach K, Alonso WJ, Charu V, Tamerius J, Simonsen L, Miller MA, Viboud C. et al. 2013. Latitudinal variations in seasonal activity of influenza and respiratory syncytial virus (RSV): a global comparative review.*PLoS One* 8(2):e54445. doi: 10.1371/journal.pone.0054445.

4. Caini S, Andrade W, Badur S, Balmaseda A, Barakat A, Bella A, Bimohuen A, Brammer L, Bresee J, Bruno A, Castillo L, Ciblak MA, Clara AW, Cohen C, Cutter J, Daouda C, de Lozano C, De Mora D, Dorji K, Emukule GO, Fasce RA, Feng L, Ferreira de Almeida WA, Guiomar R, Heraud JM, Holubka O, Huang QS, Kadjo HA, Kiyanbekova L, Kosasih H, Kusznierz G, Lara J, Li M, Lopez L, Mai Hoang PV, PessanhaHenriques CM, Matute ML, Mironenko A, Moreno B, Mott JA, Njouom R, Nurhayati, Ospanova A, Owen R, Pebody R, Pennington K, Puzelli S, Quynh Le MT, Razanajatovo NH, Rodrigues A, Rudi JM, Tzer Pin Lin R, Venter M, Vernet MA, Wangchuk S, Yang J, Yu H, Zambon M, Schellevis F, Paget J; Global Influenza B Study. 2016.Temporal Patterns of Influenza A and B in Tropical and Temperate Countries: What Are the Lessons for Influenza Vaccination? *PLoS ONE* 11(3): e0152310.

402 doi:10.1371/journal.pone.0152310

403 5. Caini S, Alonso WJ, Balmaseda A, Bruno A, Bustos P, Castillo L, de Lozano C, de Mora
404 D, Fasce RA, Ferreira de Almeida WA, Kusznierz GF, Lara J, Matute ML, Moreno B, Pessanha
405 Henriques CM, Rudi JM, El-Guerche Séblain C, Schellevis F, Paget J; Global Influenza B Study
406 group–Latin America.2017.Characteristics of seasonal influenza A and B in Latin America:
407 Influenza surveillance data from ten countries. *PLoS ONE* 12(3): e0174592. https://doi.org/
408 10.1371/journal.pone.0174592

409 6. Cao Zhd, ZENG Dajun, WANG Feiyue, WANG Quanyi, WANG Xiaoli, WANG Jiaojiao,
410 ZHENG Xiaolong. 2010.Weather Conditions and Spatio-Temporal Spreading Risk of the
411 Beijing2009 Influenza A(H1N1) Epidemic. Science &Technology. 28(8):26-32.(Chinese)

412 7.Cazelles B, Chavez M, Magny GC, Guégan JF, Hales S. 2007. Time-dependent spectral
413 analysis of epidemiological time-series with wavelets. J R SocInterface 4(15):625-36.

414 8. Eric K. W. Ng，Johnny C. L. Chan. 2012.Geophysical Applications of Partial Wavelet
415 Coherence and Multiple Wavelet Coherence. *Journal of Atmospheric & Oceanic*
416 *Technology* 29 (12) :1845–1853

417 9. Grinsted, A.， Moore, J. C.， Jevrejeva, S.2004. Application of the cross wavelet transform
418 and wavelet coherence to geophysical time series.*Nonlinear Processes in*
419 *Geophysics* 11 (5/6) :561-56**6**

420 10. Hope-Simpson, R.E., 1981. The role of season in the epidemiology of influenza.J.Hyg.
421 (Lond.) 86, 35–47.

422 11. Iuliano AD, Roguski KM, Chang HH, Muscatello DJ, Palekar R, Tempia S, Cohen C, Gran
423 JM, Schanzer D, Cowling BJ, Wu P, Kyncl J, Ang LW, Park M, Redlberger-Fritz M, Yu H,
424 Espenhain L, Krishnan A, Emukule G, van Asten L, Pereira da Silva S, Aungkulanon S,
425 Buchholz U, Widdowson MA, Bresee JS.2018. Global Seasonal Influenza-
426 associated Mortality Collaborator Network. *Lancet*. 391(10127):1285-1300. doi: 10.1016/S0140-
427 6736(17)33293-2
428 12. K.C. Chong, T.C. Lee and J. Chen , Wisely S.C. Choy , Mel Krajden , Hamid Jalal , Lance
429 Jennings, Burmaa Alexander , Hong Kai Lee , Pieter Fraaij , Avram Levy , Apple C.M. Yeung c ,
430 Sarah Tozer, Steven Y.F. Lau , Katherine M. Jia , Julian W.T. Tang , David S.C. Hui , Paul K.S.
431 Chan.2019. Association between meteorological variations and activities of influenza A and B
432 across different climate zones: A multi-region modelling analysis across the globe, Journal of
433 Infection, https://doi.org/10.1016/ j.jinf.2019.09.013
434 13. Kissling E, Valenciano M, Larrauri A, Oroszi B, Cohen JM, Nunes B, Pitigoi D, Rizzo
435 C, Rebolledo J, Paradowska-Stankiewicz I, Jiménez-Jorge S, Horváth JK, Daviaud I, Guiomar
436 R, Necula G, Bella A, O'Donnell J, Głuchowska M, Ciancio BC, Nicoll A, Moren A.. 2013.Low
437 and decreasing vaccine effectiveness against influenza A(H3) in 2011/12 among vaccination
438 target groups in Europe: results from the I-MOVE multicentre case-control study. Euro
439 Surveill.18(5): pii: 20390
440 14. Kristoufek L.2014. What are the main drivers of the Bitcoin price? Evidence from wavelet
441 coherence analysis.*Plos One* 10 (4) :e0123923
442 15. Jing Li, YuhanRao, Qinglan Sun, XiaoxuWu, Jiao Jin, Yuhai Bi, Jin Chen, Fumin Lei,

443 Qiyong Liu, ZiyuanDuan, Juncai Ma, George F.Gao, Di Liu1, &Wenjun Liu. 2015.Identification
444 of climate factors related to human infection with avian influenza A H7N9 and H5N1 viruses in
445 China. *Sci Rep*. 5:18094. doi: 10.1038/srep18094.
446 16. Liu XX, Li Y, Zhu Y, Zhang J, Li X, Zhang J, Zhao K, Hu M, Qin G, Wang
447 XL.2017.Seasonal pattern of influenza activity in a subtropical city, China, 2010–2015.
448 Scientific Reports 7 (1) :17534
449 17. Lofgren E, Fefferman NH, Naumov YN, Gorski J, Naumova EN. 2007.Influenza seasonality:
450 underlying causes and modeling theories. *J. Virol.*81:5429 –5436.
451 http://dx.doi.org/10.1128/JVI.01680-06.
452 18. Lowen AC, Steel J. 2014. Roles of Humidity and Temperature in Shaping Influenza
453 Seasonality. *Journal of Virology*. 88(14):7692-5. doi: 10.1128/JVI.03544-13.
454 19.Mahamat A, Dussart P, Bouix A, Carvalho L, Eltges F, Matheus S, Miller MA, Quenel
455 P, Viboud C.2013.Climatic drivers of seasonal influenza epidemics in French Guiana, 2006-2010.
456 *J Infect.*67(2):141-7. doi: 10.1016/j.jinf.2013.03.018.
457 20.Monamele GC, Vernet MA, Nsaibirni RFJ, Bigna JJR, Kenmoe S, Njankouo MR, Njouom R.
458 2017. Associations between meteorological parameters and influenza activity in a subtropical
459 country: Case of five sentinel sites in YaoundeÂ-Cameroon. *PLoS ONE* 12(10): e0186914.
460 https://doi.org/10.1371/
461 21. Murray EJ, Morse SS. 2011.Seasonal oscillation of human infection with influenza A/H5N1
462 in Egypt and Indonesia. *PLoS One.* 6(9):e24042 doi: 10.1371/journal.pone.0024042
463 22. Noti JD, Blachere FM, McMillen CM, Lindsley WG, Kashon ML, Slaughter DR, Beezhold

464 DH.2013. High humidity leads to loss of infectious influenza virus from simulated coughs. PLoS
465 One. 2013;8(2):e57485. doi: 10.1371/journal.pone.0057485
466 23. Onozuka D, Hagihara A.2015. All-cause and cause-specific risk of emergency transport
467 attributable to temperature: A nationwide study. *Medicine*. 94:e2259.
468 24. Pebody R, Andrews N, McMenamin J, Durnall H, Ellis J, Thompson CI, Robertson
469 C, Cottrell S, Smyth B, Zambon M, Moore C, Fleming DM, Watson JM. Vaccine effectiveness
470 of 2011/12 trivalent seasonal influenza vaccine in preventing laboratory-confirmed influenza in
471 primary care in the United Kingdom: evidence of waning intra-seasonal protection. *Euro Surveill.*
472 2013; 18(5): 25-32
473 25. Peci A, Winter AL, Li Y, Gnaneshan S, Liu J, Mubareka S, Gubbay JB.2019. Effects of
474 Absolute Humidity, Relative Humidity, Temperature, and Wind Speed on Influenza Activity in
475 Toronto, Ontario, Canada. Appl Environ Microbiol. 85(6). pii: e02426-18. doi:
476 10.1128/AEM.02426-18.
477 26. Pica N, Bouvier NM. 2012. Environmental Factors Affecting the Transmission of
478 Respiratory Viruses. *CurrOpinVirol*. 2(1):90–5. doi: 10.1016/j.coviro.2011.12.003
479 27.Soebiyanto RP, Adimi F, Kiang RK. 2010.
480 Modeling and predicting seasonal influenza transmission in warm regions using climatological
481 parameters.*PLoSOne*. 5(3):e9450. doi: 10.1371/journal.pone.0009450.
482 28. Shaman J, Goldstein E, Lipsitch M.2011.Absolute humidity and pandemic
483 Versus epidemic influenza.*Am J Epidemiol* 173: 127–135.
484 29. Shaman J, Kohn M .2009. Absolute humidity modulates influenza survival,

485 transmission, and seasonality.*ProcNatlAcadSci USA* 106: 3243–3248.

486 30. Shaman J, Pitzer VE, Viboud C, Grenfell BT, Lipsitch M. 2010.Absolute humidity and the
487 seasonal onset of influenza in the continental United States. *PLo S Biol* 8: e1000316.
488 doi:10.1371/journal.pbio.1000316

489 31.Sundell N, Andersson LM, Brittain-Long R, Lindh M, Westin J. 2016. A four year seasonal
490 survey of the relationship between outdoor climate and epidemiology of viral respiratory tract
491 infections in a temperate climate. J ClinVirol. 84:59-63. doi: 10.1016/j.jcv.2016.10.005.

492 32.Sun JY, SUN Xiao-yu, XIAO Zheng. 2018. Correlation between meteorological parameters
493 and influenza activity in Xicheng District of Beijing.Occup and Health 34(20):2811-
494 2814.(Chinese)

495 33.Tamerius JD, Shaman J, Alonso WJ, Bloom-Feshbach K, Uejio CK, Comrie A, Viboud C. et
496 al.2013.Environmental predictors of seasonal influenza epidemics across temperate and tropical
497 climates.*PLoSPathog*. 9(3):e1003194.

498 34. Tamerius J, Nelson M, Zhou S, Viboud C, Miller M, Alonso W. 2011. Global influenza
499 seasonality: reconciling patterns across temperate and tropical regions. *Environ Health Perspect.*
500 119(4):439-45. doi: 10.1289/ehp.1002383.

501 35.Tamerius J, Uejio C, Koss J.2019. Seasonal characteristics of influenza vary regionally across
502 US. *PLoS One.* 14(3):e0212511. doi: 10.1371/journal.pone.0212511

503 36.Thai PQ, Choisy M, Duong TN, Thiem VD, Yen NT, Hien NT, Weiss DJ, Boni MF, Horby P.
504 2015. Seasonality of absolute humidity explains seasonality of influenza-like illness in Vietnam.
505 *Epidemics.*13:65-73. doi: 10.1016/j.epidem.2015.06.002.

506 37. Wu Z, Sun X, Chu Y, Sun J, Qin G, Yang L, Qin J, Xiao Z, Ren J, Qin D, Wang X, Zheng X.
507 2016. Coherence of Influenza Surveillance Data across Different Sources and Age Groups,
508 Beijing, China, 2008-2015. PLoS ONE 11(12): e0169199. doi:10.1371/journal.pone.0169199
509 38. Xiao H, Lin XL, Dai XY, Gao LD, Chen BY, Zhang XX, Zhu PJ, Tian HY.
510 2012.Study on sensitivity of climatic factors on influenza A (H1N1) based on classification and
511 regression tree and wavelet analysis. *Zhonghua Yu Fang Yi Xue Za Zhi (In Chinese)*. 46(5):430-
512 5.
513 39. Yang W, Elankumaran S, Marr LC. 2012. Relationship between humidity and influenza A
514 viability in droplets and implications for influenza's seasonality. PLOS ONE 7:e46789
515 40..Yang XT Liu Dongpeng, He Jian, Gou Faxiang, Liu Haixia, ZhengYunhe, Wei
516 Kongfu, Cheng Yao, Liu Xinfeng. 2019.Classification and regression tree model study on
517 correlation between influenza epidemic and meteorological factors indifferent areas of Gansu,
518 2010 to 2016.DISEASE SURVEILLANCE, 34(5):440-445 (Chinese)
519 41. Yu H, Alonso WJ, Feng L, Tan Y, Shu Y, Yang W, Viboud C. 2013. Characterization of
520 Regional Influenza Seasonality Patterns in China and Implications for Vaccination Strategies:
521 Spatio-Temporal Modeling of Surveillance Data.*PLo S Med* 10(11): e1001552.
522 doi:10.1371/journal.pmed.1001552
523
524
525
526

527

528

529

530

531

532

533

534

535

536

537

538 **Figure Legends**

539 **Figure 1 The composite influenza virus activity in Jinan, Eastern China, 2013-2016.**

540 (A) The weekly positive rates of all influenza viruses combined and week distribution of
541 influenza virus A (A(H3N2) and A(H1N1)pdm09) and influenza virus B (B/Yamagata and
542 B/Victoria) (B) Wavelet power spectrum of the positive rate of all influenza viruses combined.
543 The 5% significant level against red noise is shown as a thick black curve. The cone of influence,
544 which indicates the region affected by edge effects, is shown with a lighter shade. The color code
545 for power ranges from pink (low power) to white (high power). X-axis denotes the time and Y-
546 axis represents frequency periods.

547

548

549 **Figure 2 Seasonal distribution and wavelet power spectrum of influenza types or**
550 **subtypes.**

551 (**A)** The weekly positive rate and week distribution of influenza virus A(H3N2).

552 (**B)** Wavelet power spectrum of the positive rate of influenza virus A(H3N2).

553 (C) The weekly positive rate and week distribution of influenza virus A(H1N1)pdm09.

554 (**D)** Wavelet power spectrum of the positive rate of influenza virus A(H1N1)pdm09.

555 (**E)** The weekly positive rate and week distribution of influenza virus B.

556 (**F)** Wavelet power spectrum of the positive rate of influenza virus B.

557 The 5% significant level against red noise is shown as a thick black curve. The cone of influence,
558 which indicates the region affected by edge effects, is shown with a lighter shade. The color code
559 for power ranges from pink (low power) to white (high power). X-axis denotes the time and y-
560 axis represents frequency periods.

561

562

563 **Figure 3 The time-series results of the positive rate of influenza virus and climate factors in**
564 **Jinan, 2013－2016.**

565 (A) atmospheric pressure. (B) average temperature. (C) relative humidity. (D) absolute humidity.
566 (E) accumulated rainfall. (F) wind speed. (G) sunshine duration. (H) influenza positive rate.

567

568

Figure 4 The wavelet transform coherence of influenza virus A(H3N2) and different climate parameters.

Wavelet transform coherence is represented by a colored contour: the whiter the color is, the higher the local correlation in the time-frequency periods space (with time on the x-axis and frequencies on the y-axis). The matching of colors and correlation levels is represented by the scale on the right hand side of the upper graph. The 5% significant level against red noise is shown as a thick black curve. The cone of influence, which indicates the region affected by edge effects, is shown with a lighter shade black line. The color code for power ranges from pink (low power) to white (high power). The phase difference between the two series is indicated by arrows. Arrows pointing to the right mean that the variables are in phase. Arrows pointing to the left mean that the variables are out of phase. The down arrows show that climate factor is leading. The up arrows mean that influenza virus is leading. In phase indicate that variables will be having cyclical effect on each other and out of phase or anti-phase shows that variable will be having ant-cyclical effect on each other.

(A) influenza virus A(H3N2) and atmospheric pressure. (B) influenza virus A(H3N2) and average temperature. (C) influenza virus A(H3N2) and relatively humidity. (D) influenza virus A(H3N2) and absolute humidity. (E) influenza virus A(H3N2) and rainfall. (F) influenza virus A(H3N2) and wind speed.

Figure 5 The wavelet transform coherence of influenza virus A(H1N1)pdm09 and different

climate parameters.

Wavelet transform coherence is represented by a colored contour: the whiter the color is, the higher the local correlation in the time-frequency periods space (with time on the x-axis and frequencies on the y-axis). The matching of colors and correlation levels is represented by the scale on the right hand side of the upper graph. The 5% significant level against red noise is shown as a thick black curve. The cone of influence, which indicates the region affected by edge effects, is shown with a lighter shade black line. The color code for power ranges from pink (low power) to white (high power). The phase difference between the two series is indicated by arrows. Arrows pointing to the right mean that the variables are in phase. Arrows pointing to the left mean that the variables are out of phase. The down arrows show that climate factor is leading. The up arrows mean that influenza virus is leading. In phase indicate that variables will be having cyclical effect on each other and out of phase or anti-phase shows that variable will be having ant-cyclical effect on each other.

(A) influenza virus A(H1N1)pdm09 and atmospheric pressure. (B) influenza virus A(H1N1)pdm09 and average temperature. (C) influenza virus A(H1N1)pdm09 and relatively humidity. (D) influenza virus A(H1N1)pdm09 and absolute humidity. (E) influenza virus A(H1N1)pdm09 and rainfall.

Figure 6 The wavelet transform coherence of influenza virus B and different climate parameters.

611 Wavelet transform coherence is represented by a colored contour: the whiter the color is, the
612 higher the local correlation in the time-frequency periods space (with time on the x-axis and
613 frequencies on the y-axis). The matching of colors and correlation levels is represented by the
614 scale on the right hand side of the upper graph. The 5% significant level against red noise is
615 shown as a thick black curve. The cone of influence, which indicates the region affected by edge
616 effects, is shown with a lighter shade black line. The color code for power ranges from pink (low
617 power) to white (high power). The phase difference between the two series is indicated by
618 arrows. Arrows pointing to the right mean that the variables are in phase. Arrows pointing to the
619 left mean that the variables are out of phase. The down arrows show that climate factor is leading.
620 The up arrows mean that influenza virus is leading. In phase indicate that variables will be
621 having cyclical effect on each other and out of phase or anti-phase shows that variable will be
622 having ant-cyclical effect on each other.
623 (A) influenza Virus B and atmospheric pressure. (B) influenza Virus B and average temperature.
624 (C) influenza Virus B and relatively humidity. (D) influenza Virus B and absolute humidity. (E)
625 influenza Virus B and rainfall
626
627
628 **Figure 7 Multiple Wavelet Coherence of Influenza virus A(H3N2) and climate factors.**
629 The 5% significant level against red noise is shown as a thick black curve. The cone of influence,
630 which indicates the region affected by edge effects, is shown with a lighter shade. The color code
631 for power ranges from pink (low power) to white (high power).

(A) influenza virus A(H3N2), temperature and atmospheric pressure.

(B) influenza virus A(H3N2), temperature and AH.

(C) influenza virus A(H3N2), temperature and RH.

(D) influenza virus A(H3N2), AH and atmospheric pressure.

(E) influenza virus A(H3N2), AH and RH.

(F) influenza virus A(H3N2), RH and atmospheric pressure.

Figure 8 Multiple Wavelet Coherence of Influenza virus A(H1N1)pdm09 and climate factors.

The 5% significant level against red noise is shown as a thick black curve. The cone of influence, which indicates the region affected by edge effects, is shown with a lighter shade. The color code for power ranges from pink (low power) to white (high power)..

(A) influenza virus A(H1N1)pdm09, temperature and atmospheric pressure.

(B) influenza virus A(H1N1)pdm09, temperature and AH.

(C) influenza virus A(H1N1)pdm09, temperature and RH.

(D) influenza virus A(H1N1)pdm09, AH and atmospheric pressure.

(E) influenza virus A(H1N1)pdm09, AH and RH.

(F) influenza virus A(H1N1)pdm09, RH and atmospheric pressure.

653 **Figure 9 Multiple Wavelet Coherence of Influenza virus B and climate factors.**

654 The 5% significant level against red noise is shown as a thick black curve. The cone of influence,

655 which indicates the region affected by edge effects, is shown with a lighter shade. The color code

656 for power ranges from pink (low power) to white (high power).

657 (A) influenza virus B, temperature and atmospheric pressure.

658 (B) influenza virus B, temperature and AH.

659 (C) influenza virus B, temperature and RH.

660 (D) influenza virus B, AH and atmospheric pressure.

661 (E) influenza virus B, AH and RH.

662 (F) influenza virus B, RH and atmospheric pressure.

663

Table 1(on next page)

Table 1 Description of weekly climatic factors in Jinan, 2013-2016

1 **Table 1 Description of weekly climatic factors in Jinan, 2013-2016**

Variables	Minimum	Maximum	Mean	Standard deviation
Atmospheric pressure (hPa)	979.4	1013.4	996.5	8.5
Mean temperature (℃)	-6.4	30.6	15.3	9.9
Relative humidity (%)	23.3	91.7	56.4	14.6
Absolute humidity (g/m^3)	1.5	17.9	7.5	4.5
Wind speed (m/s)	1.0	4.5	2.5	0.6
Sunshine duration (h)	5.3	77.9	37.5	17.1
Rainfall (mm)	0	102.4	5.1	13.7
Influenza A(H1N1)pdm09 virus (number)	0	37	1.8	5.5
Influenza A(H3N2)virus (number)	0	24	1.4	4.0
Influenza virus B(number)	0	28	1.2	3.3

2

Table 2(on next page)

Table 2 The correlation between positive rate of different influenza virus types or subtypes and different climatic factors from 2013 to 2016

[a] the strength of the association is interpreted as weak when coefficients are in the range of 0.1 to 0.3, medium when the coefficients are in the range of 0.3 to 0.7, and strong when the coefficients are in the range of 0.7 to 1.0, according to the report of K.C. Chong et al (2019)

[*]p□0.05 [**] p□0 .01

Table 2 The correlation between positive rate of different influenza virus types or subtypes and different climatic factors from 2013 to 2016[a]

Variables	Atmospheric pressure	Mean temperature	Relative humidity	Absolute humidity	Wind speed	Sunshine duration	Rainfall
Influenza A(H1N1)pdm09	0.521**	-0.632**	-0.245**	-0.623**	-0.020	-0.132	-0.240**
Influenza A(H3N2) virus	0.539**	-0.522**	-0.139**	-0.487**	-0.164*	-0.122	-0.285**
Influenza virus B	0.377**	-0.450**	-0.292**	-0.494**	0.097	-0.063	-0.277**

[a] the strength of the association is interpreted as weak when coefficients are in the range of 0.1 to 0.3, medium when the coefficients are in the range of 0.3 to 0.7, and strong when the coefficients are in the range of 0.7 to 1.0, according to the report of K.C. Chong et al (2019)

*p＜0. 05 ** p＜0. 01

Figure 1

The composite influenza virus activity in Jinan, Eastern China, 2013-2016.

(A) The weekly positive rates of all influenza viruses combined and week distribution of influenza virus A (A(H3N2) and A(H1N1)pdm09) and influenza virus B (B/Yamagata and B/Victoria) (B) Wavelet power spectrum of the positive rate of all influenza viruses combined. The 5% significant level against red noise is shown as a thick black curve. The cone of influence, which indicates the region affected by edge effects, is shown with a lighter shade. The color code for power ranges from pink (low power) to white (high power). X-axis denotes the time and Y-axis represents frequency periods.

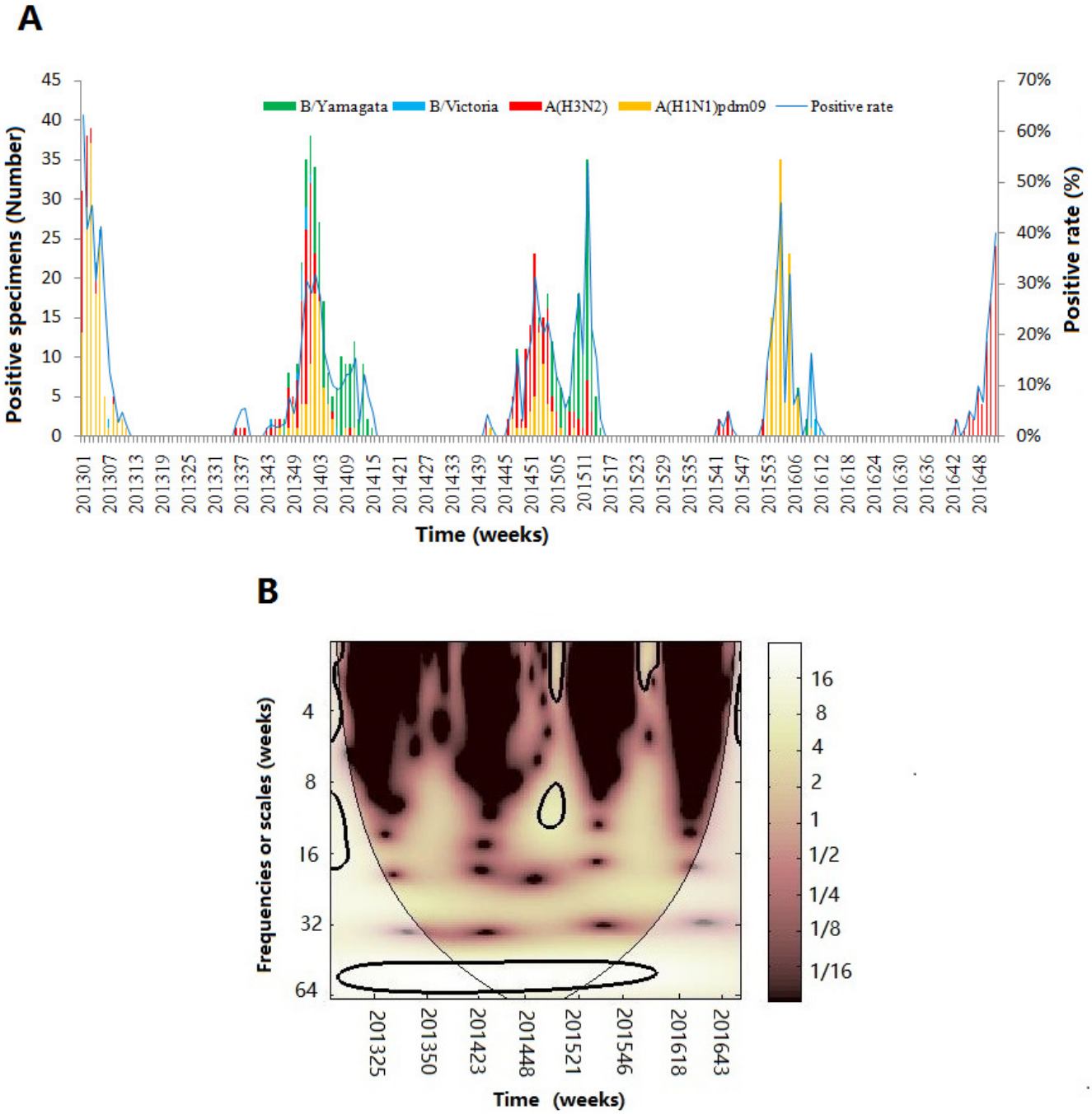
A
B/Yamagata
B/Victoria
A(H3N2)
A(H1N1)pdm09
Positive rate
Positive specimens (Number)
Positive rate (%)
Time (weeks)
B
Frequencies or scales (weeks)
Time (weeks)

Figure 2

Seasonal distribution and wavelet power spectrum of influenza types or subtypes

(**A)** The weekly positive rate and week distribution of influenza virus A(H3N2). (**B)** Wavelet power spectrum of the positive rate of influenza virus A(H3N2). (C) The weekly positive rate and week distribution of influenza virus A(H1N1)pdm09. (**D)** Wavelet power spectrum of the positive rate of influenza virus A(H1N1)pdm09. (**E)** The weekly positive rate and week distribution of influenza virus B. (**F)** Wavelet power spectrum of the positive rate of influenza virus B. The 5% significant level against red noise is shown as a thick black curve. The cone of influence, which indicates the region affected by edge effects, is shown with a lighter shade. The color code for power ranges from pink (low power) to white (high power). X-axis denotes the time and y-axis represents frequency periods.

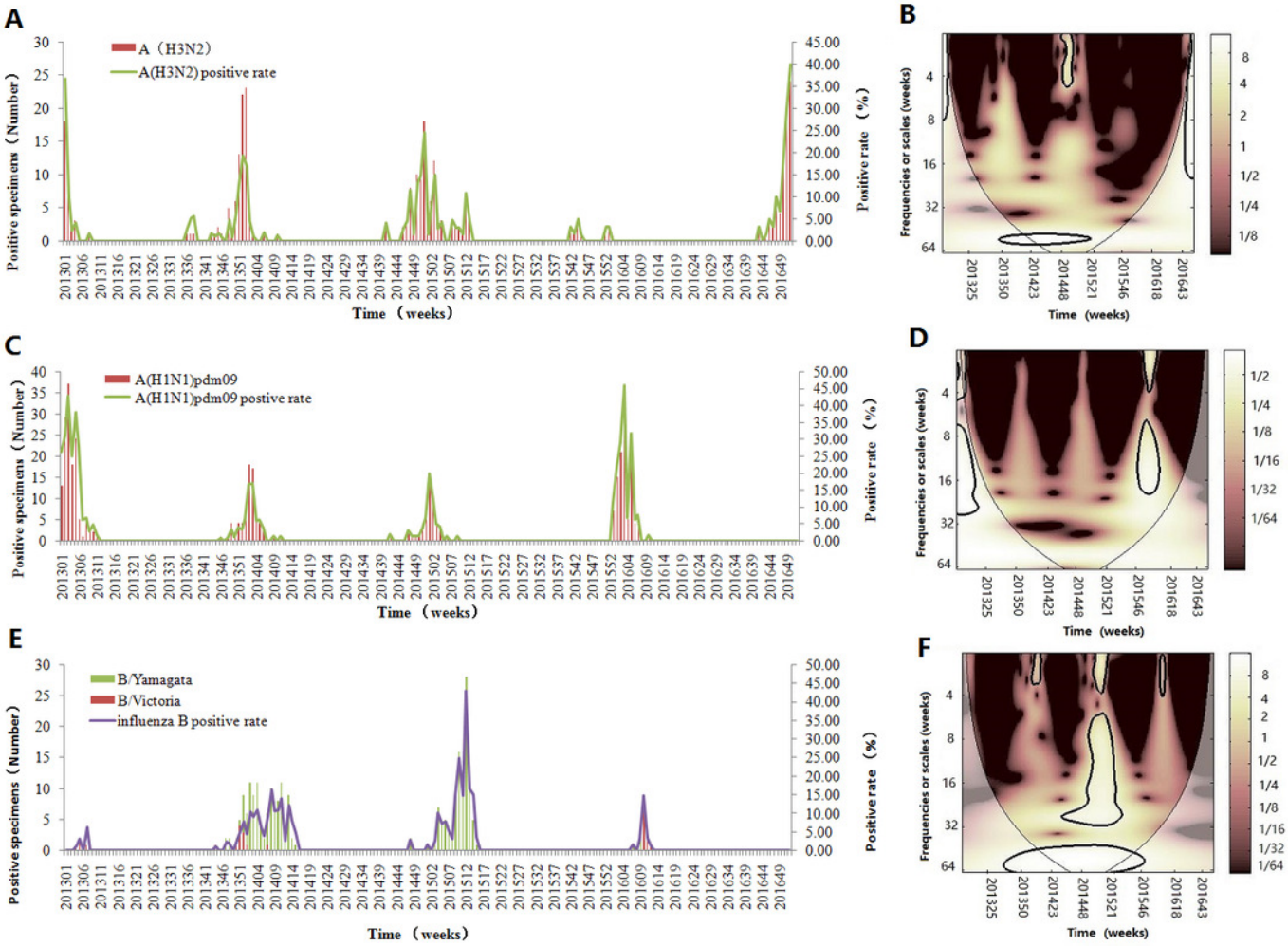
A
A（H3N2）
A(H3N2) positive rate
Positive specimens（Number）
Positive rate （%）
Time （weeks）
B
Frequencies or scales (weeks)
Time (weeks)
C
A(H1N1)pdm09
A(H1N1)pdm09 postive rate
Positive specimens（Number）
Positive rate （%）
Time （weeks）
D
Frequencies or scales (weeks)
Time (weeks)
E
B/Yamagata
B/Victoria
influenza B positive rate
Positive specimens（Number）
Positive rate （%）
Time （weeks）
F
Frequencies or scales (weeks)
Time (weeks)

Figure 3

The time-series results of the positive rate of influenza virus and climate factors in Jinan, 2013–2016

(A) atmospheric pressure. (B) average temperature. (C) relative humidity. (D) absolute humidity. (E) accumulated rainfall. (F) wind speed. (G) sunshine duration. (H) influenza positive rate.

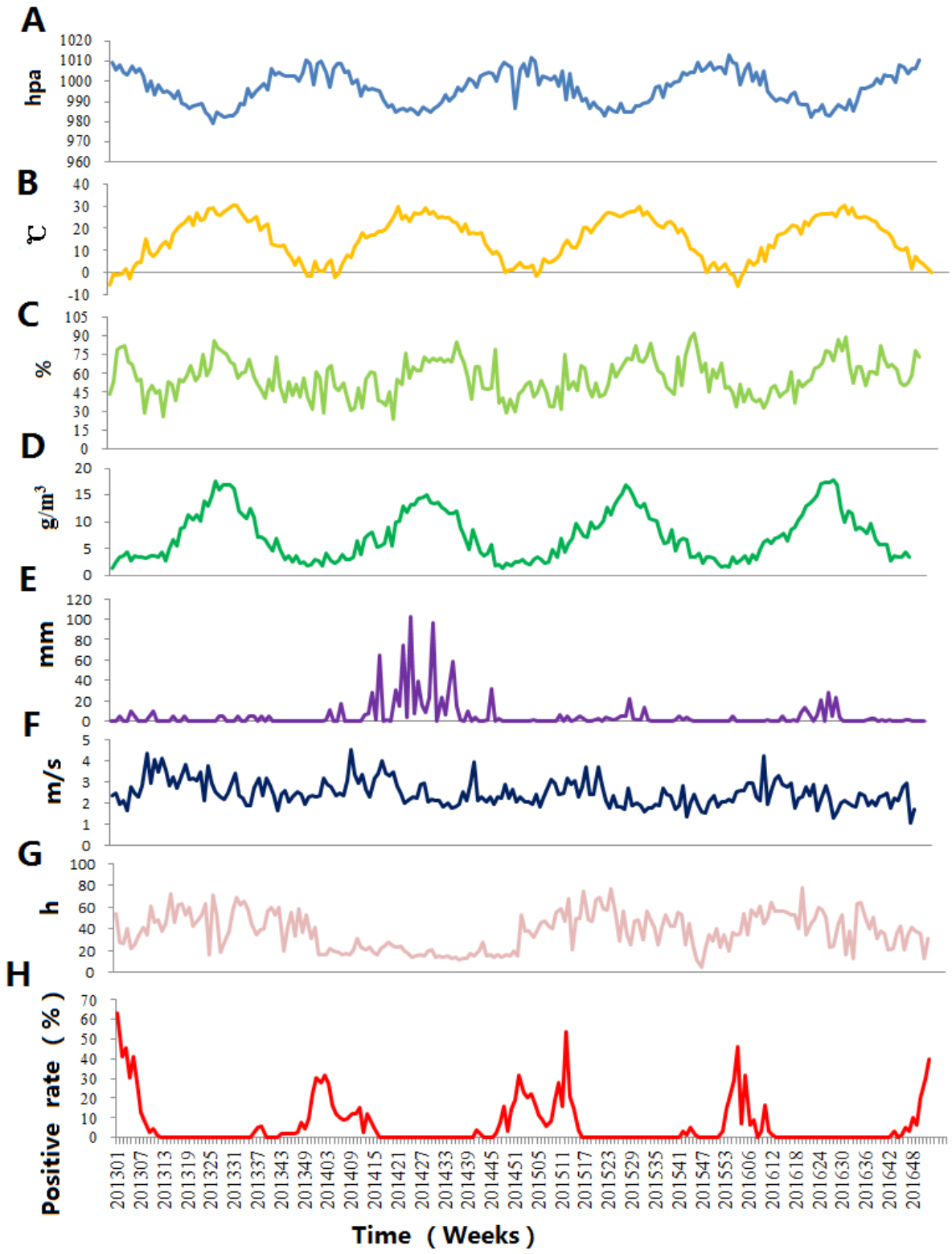
A
hpa
1020
1010
1000
990
980
970
960
B
℃
40
30
20
10
0
-10
C
%
105
90
75
60
45
30
15
0
D
g/m³
20
15
10
5
0
E
mm
120
100
80
60
40
20
0
F
m/s
5
4
3
2
1
0
G
h
100
80
60
40
20
0
H
Positive rate (%)
70
60
50
40
30
20
10
0
201301
201307
201313
201319
201325
201331
201337
201343
201349
201403
201409
201415
201421
201427
201433
201439
201445
201451
201505
201511
201517
201523
201529
201535
201541
201547
201553
201606
201612
201618
201624
201630
201636
201642
201648
Time (Weeks)

Figure 4

The wavelet transform coherence of influenza virus A(H3N2) and different climate parameters.

Wavelet transform coherence is represented by a colored contour: the whiter the color is, the higher the local correlation in the time-frequency periods space (with time on the x-axis and frequencies on the y-axis). The matching of colors and correlation levels is represented by the scale on the right hand side of the upper graph. The 5% significant level against red noise is shown as a thick black curve. The cone of influence, which indicates the region affected by edge effects, is shown with a lighter shade black line. The color code for power ranges from pink (low power) to white (high power). The phase difference between the two series is indicated by arrows. Arrows pointing to the right mean that the variables are in phase. Arrows pointing to the left mean that the variables are out of phase. The down arrows show that climate factor is leading. The up arrows mean that influenza virus is leading. In phase indicate that variables will be having cyclical effect on each other and out of phase or anti-phase shows that variable will be having ant-cyclical effect on each other. (A) influenza virus A(H3N2) and atmospheric pressure. (B) influenza virus A(H3N2) and average temperature. (C) influenza virus A(H3N2) and relatively humidity. (D) influenza virus A(H3N2) and absolute humidity. (E) influenza virus A(H3N2) and rainfall. (F) influenza virus A(H3N2) and wind speed.

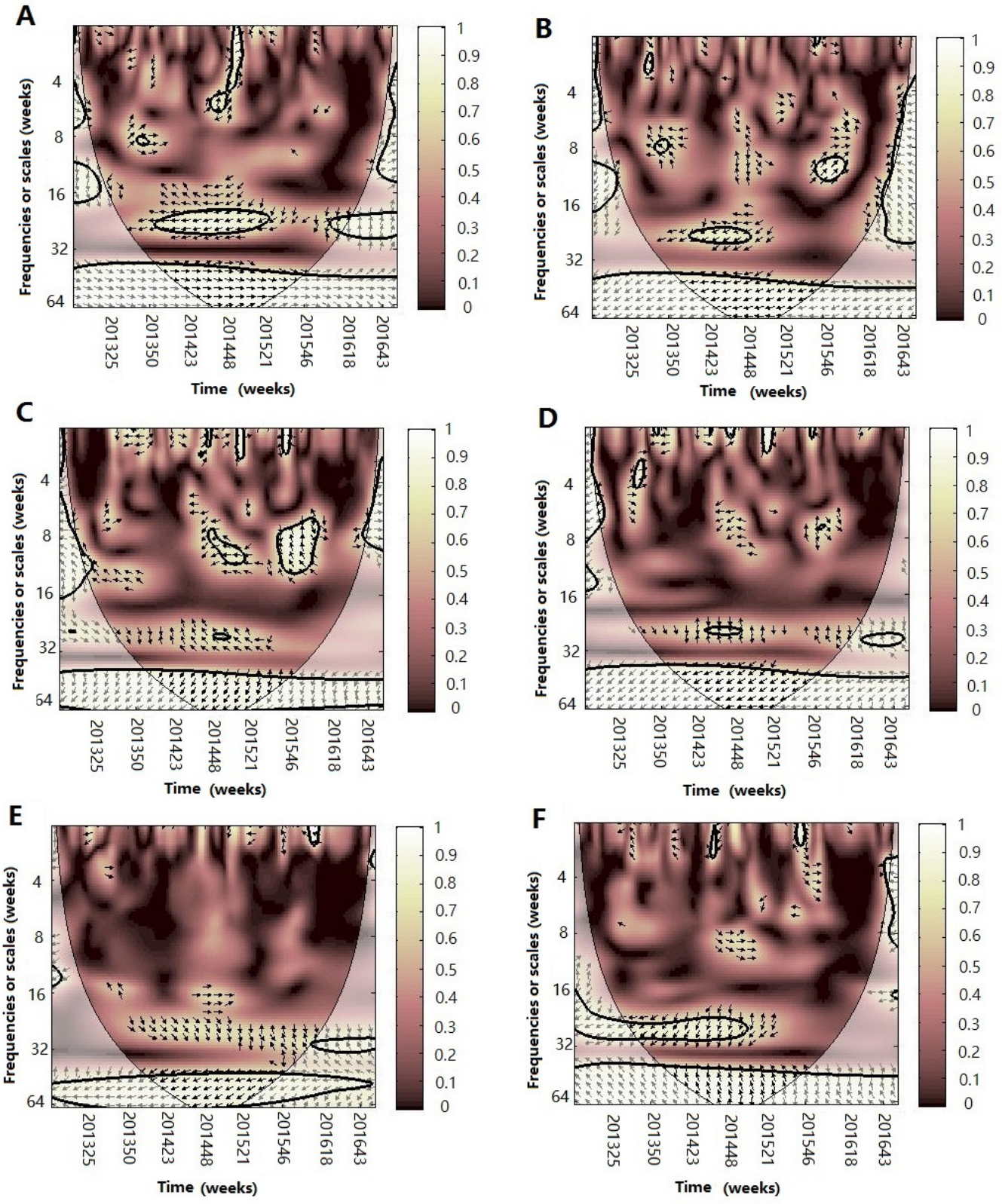
A
B
C
D
E
F
Frequencies or scales (weeks)
4
8
16
32
64
1
0.9
0.8
0.7
0.6
0.5
0.4
0.3
0.2
0.1
0
201325
201350
201423
201448
201521
201546
201618
201643
Time (weeks)

Figure 5

The wavelet transform coherence of influenza virus A(H1N1)pdm09 and different climate parameters

Wavelet transform coherence is represented by a colored contour: the whiter the color is, the higher the local correlation in the time-frequency periods space (with time on the x-axis and frequencies on the y-axis). The matching of colors and correlation levels is represented by the scale on the right hand side of the upper graph. The 5% significant level against red noise is shown as a thick black curve. The cone of influence, which indicates the region affected by edge effects, is shown with a lighter shade black line. The color code for power ranges from pink (low power) to white (high power). The phase difference between the two series is indicated by arrows. Arrows pointing to the right mean that the variables are in phase. Arrows pointing to the left mean that the variables are out of phase. The down arrows show that climate factor is leading. The up arrows mean that influenza virus is leading. In phase indicate that variables will be having cyclical effect on each other and out of phase or anti-phase shows that variable will be having ant-cyclical effect on each other. (A) influenza virus A(H1N1)pdm09 and atmospheric pressure. (B) influenza virus A(H1N1)pdm09 and average temperature. (C) influenza virus A(H1N1)pdm09 and relatively humidity. (D) influenza virus A(H1N1)pdm09 and absolute humidity. (E) influenza virus A(H1N1)pdm09 and rainfall.

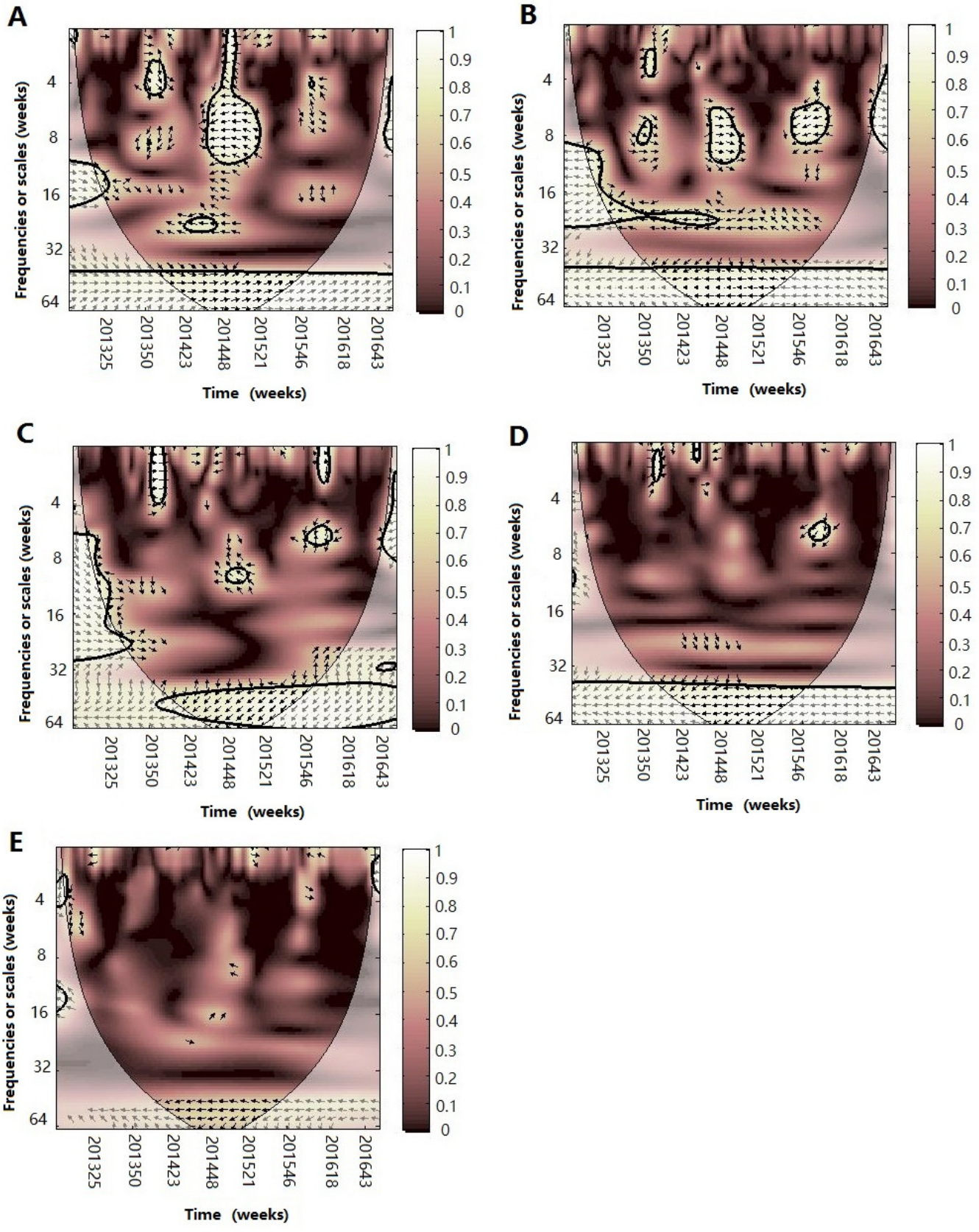
A
B
C
D
E
Frequencies or scales (weeks)
4
8
16
32
64
Time (weeks)
201325
201350
201423
201448
201521
201546
201618
201643
1
0.9
0.8
0.7
0.6
0.5
0.4
0.3
0.2
0.1
0

Figure 6

The wavelet transform coherence of influenza virus B and different climate parameters.

Wavelet transform coherence is represented by a colored contour: the whiter the color is, the higher the local correlation in the time-frequency periods space (with time on the x-axis and frequencies on the y-axis). The matching of colors and correlation levels is represented by the scale on the right hand side of the upper graph. The 5% significant level against red noise is shown as a thick black curve. The cone of influence, which indicates the region affected by edge effects, is shown with a lighter shade black line. The color code for power ranges from pink (low power) to white (high power). The phase difference between the two series is indicated by arrows. Arrows pointing to the right mean that the variables are in phase. Arrows pointing to the left mean that the variables are out of phase. The down arrows show that climate factor is leading. The up arrows mean that influenza virus is leading. In phase indicate that variables will be having cyclical effect on each other and out of phase or anti-phase shows that variable will be having ant-cyclical effect on each other. (A) influenza Virus B and atmospheric pressure. (B) influenza Virus B and average temperature. (C) influenza Virus B and relatively humidity. (D) influenza Virus B and absolute humidity. (E) influenza Virus B and rainfall

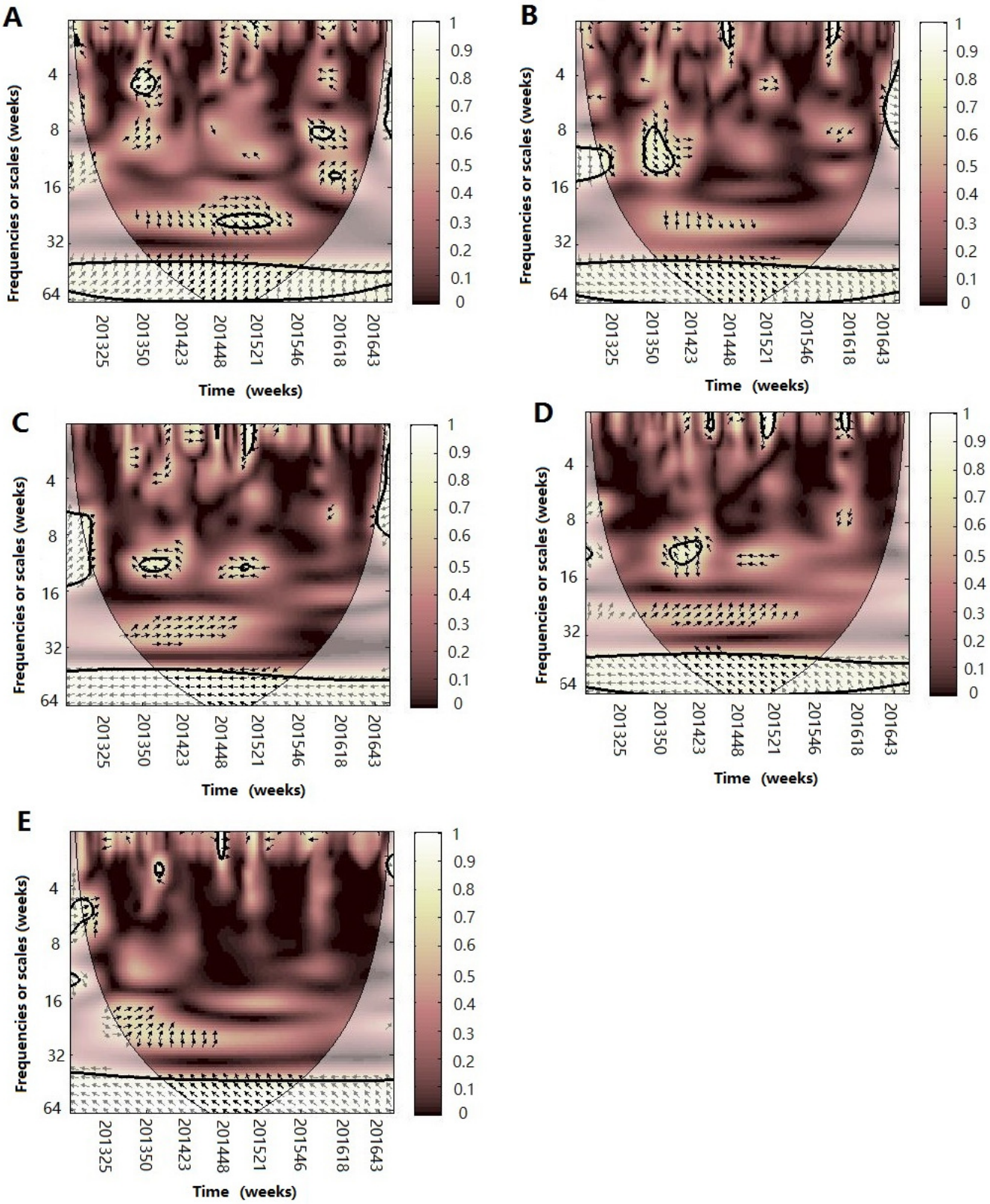
A
B
C
D
E
Frequencies or scales (weeks)
4
8
16
32
64
Time (weeks)
201325
201350
201423
201448
201521
201546
201618
201643
1
0.9
0.8
0.7
0.6
0.5
0.4
0.3
0.2
0.1
0

Figure 7

Multiple Wavelet Coherence of Influenza A(H3N2) virus and climate factors

The 5% significant level against red noise is shown as a thick black curve. The cone of influence, which indicates the region affected by edge effects, is shown with a lighter shade. The color code for power ranges from pink (low power) to white (high power). (A) influenza virus A(H3N2), temperature and atmospheric pressure. (B) influenza virus A(H3N2), temperature and AH. (C) influenza virus A(H3N2), temperature and RH. (D) influenza virus A(H3N2), AH and atmospheric pressure. (E) influenza virus A(H3N2), AH and RH. (F) influenza virus A(H3N2), RH and atmospheric pressure.

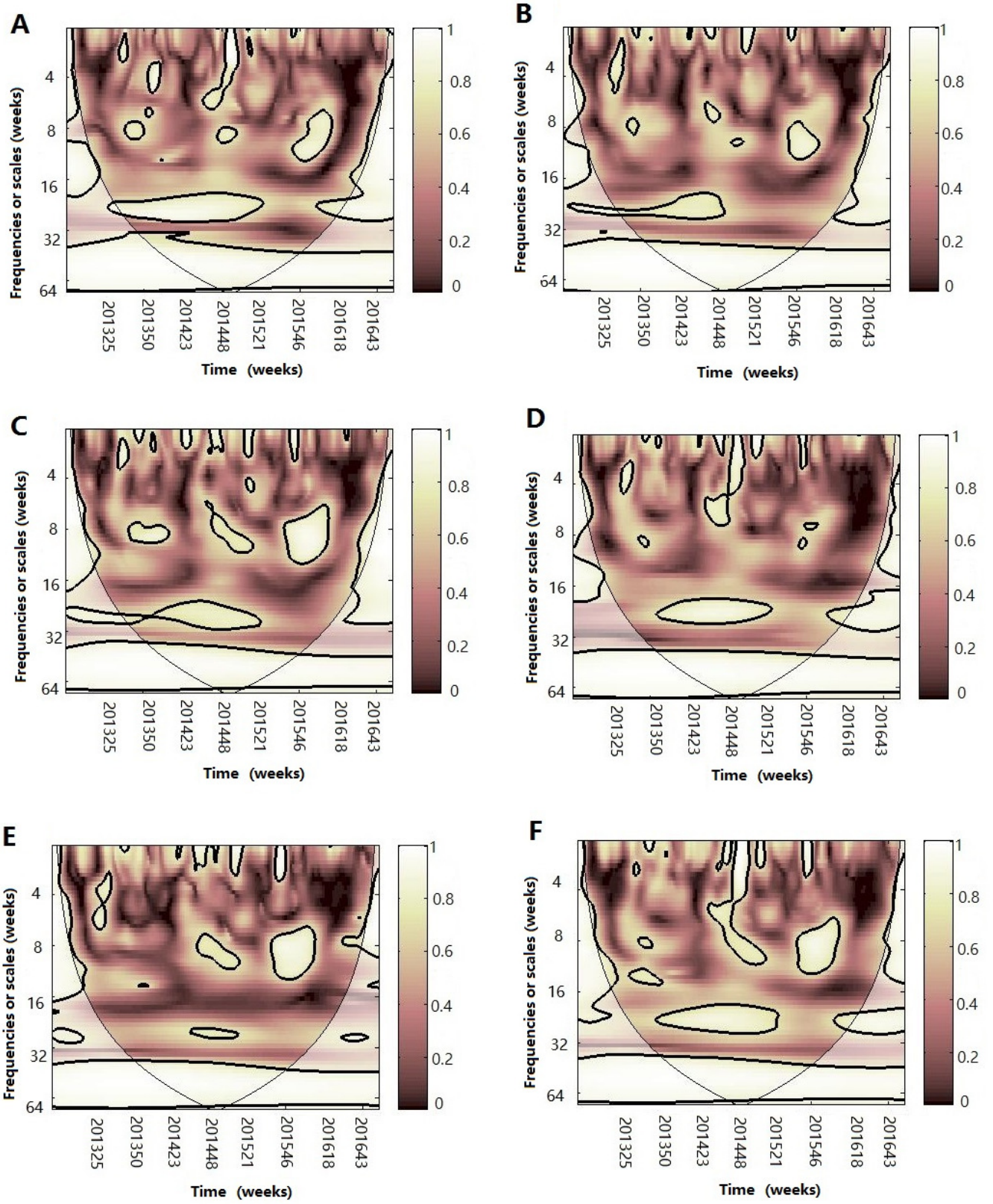
A
B
C
D
E
F
Frequencies or scales (weeks)
4
8
16
32
64
1
0.8
0.6
0.4
0.2
0
201325
201350
201423
201448
201521
201546
201618
201643
Time (weeks)

Figure 8

Multiple Wavelet Coherence of Influenza A(H1N1) pdm09 virus and climate factors

The 5% significant level against red noise is shown as a thick black curve. The cone of influence, which indicates the region affected by edge effects, is shown with a lighter shade. The color code for power ranges from pink (low power) to white (high power).. (A) influenza virus A(H1N1)pdm09, temperature and atmospheric pressure. (B) influenza virus A(H1N1)pdm09, temperature and AH. (C) influenza virus A(H1N1)pdm09, temperature and RH. (D) influenza virus A(H1N1)pdm09, AH and atmospheric pressure. (E) influenza virus A(H1N1)pdm09, AH and RH. (F) influenza virus A(H1N1)pdm09, RH and atmospheric pressure.

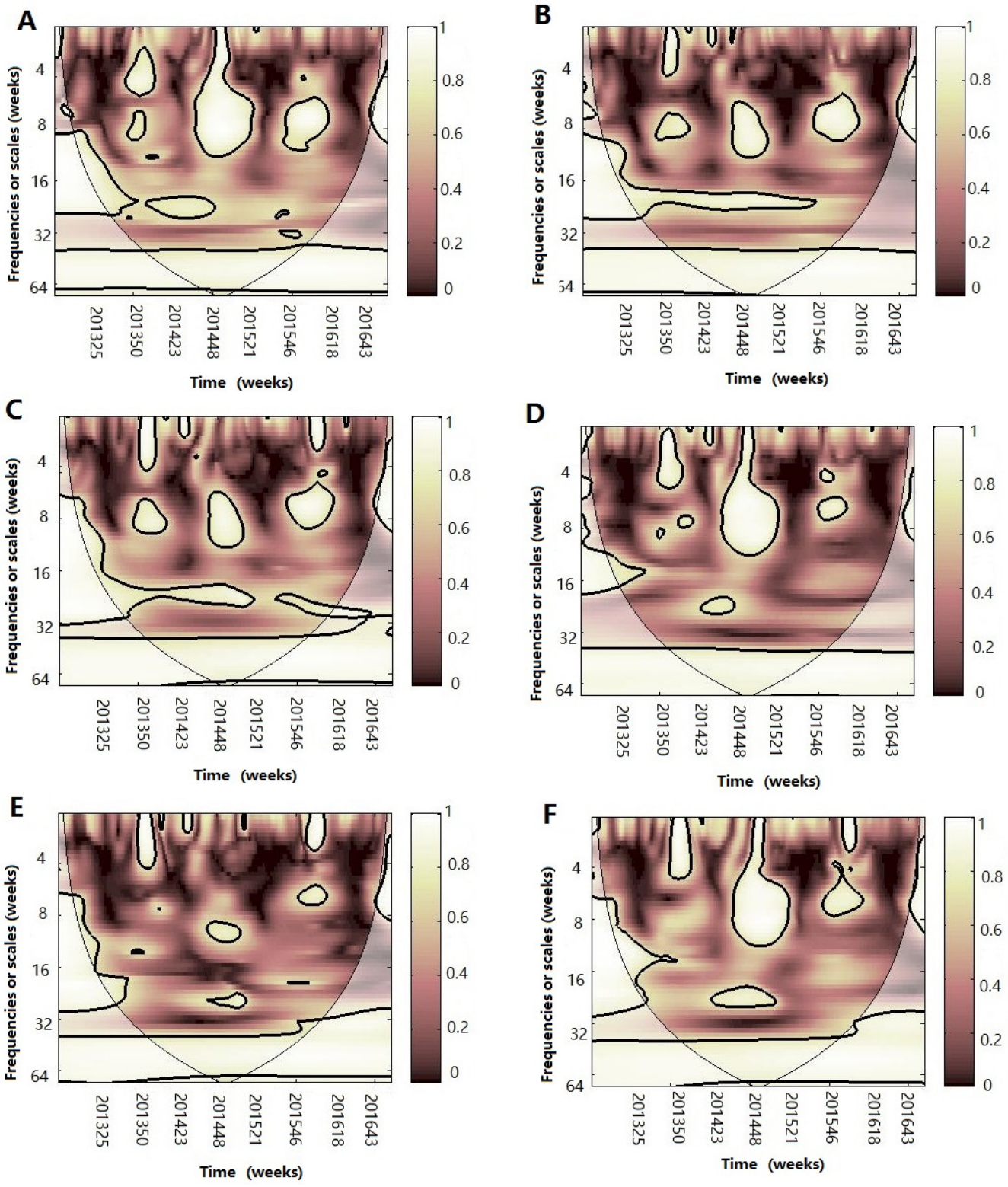
A
B
C
D
E
F
Frequencies or scales (weeks)
4
8
16
32
64
1
0.8
0.6
0.4
0.2
0
201325
201350
201423
201448
201521
201546
201618
201643
Time (weeks)

Figure 9

Multiple Wavelet Coherence of Influenza virus B and climate factors.

The 5% significant level against red noise is shown as a thick black curve. The cone of influence, which indicates the region affected by edge effects, is shown with a lighter shade. The color code for power ranges from pink (low power) to white (high power). (A) influenza virus B, temperature and atmospheric pressure. (B) influenza virus B, temperature and AH. (C) influenza virus B, temperature and RH. (D) influenza virus B, AH and atmospheric pressure. (E) influenza virus B, AH and RH. (F) influenza virus B, RH and atmospheric pressure.

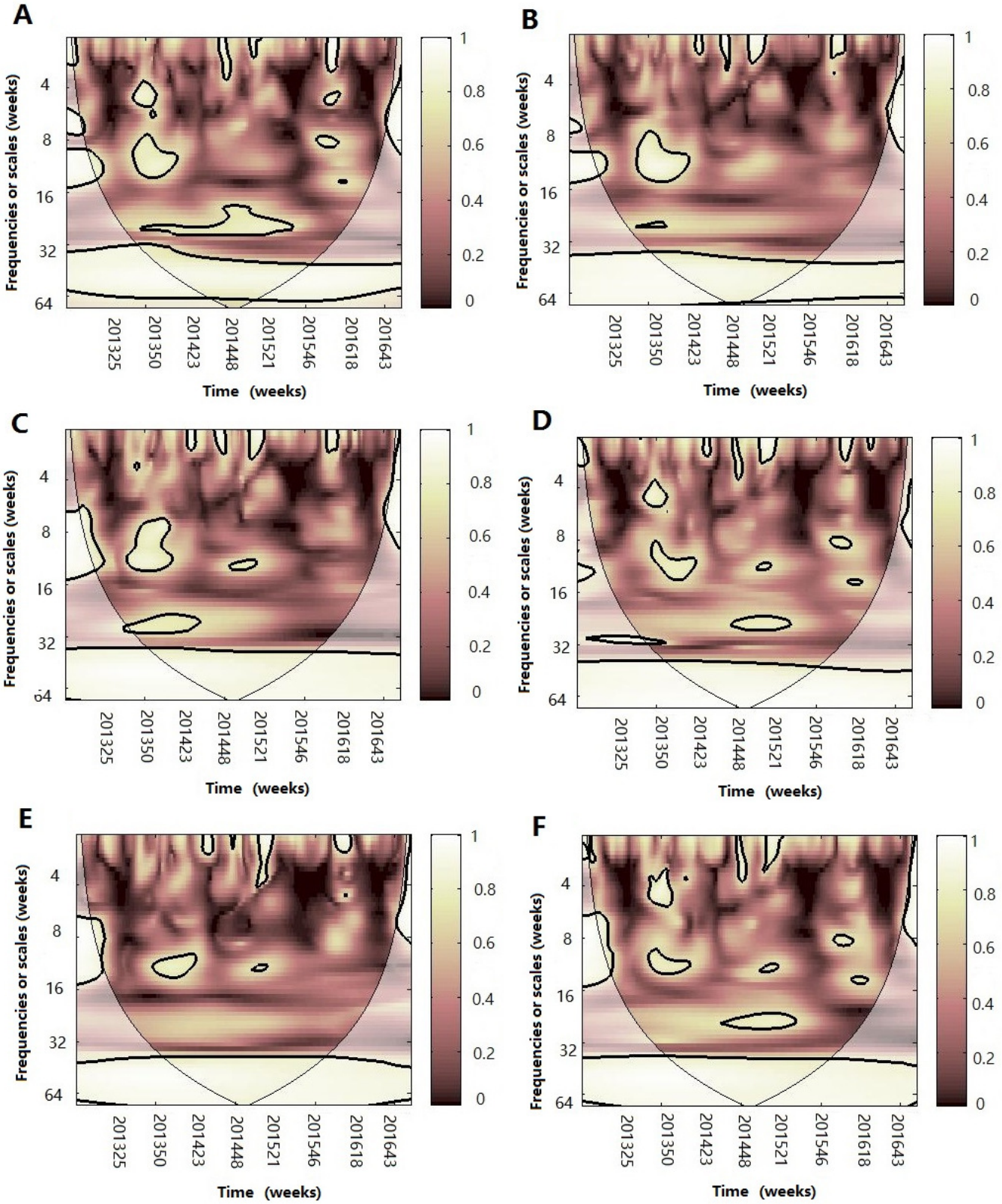
A
B
C
D
E
F
Frequencies or scales (weeks)
4
8
16
32
64
1
0.8
0.6
0.4
0.2
0
201325
201350
201423
201448
201521
201546
201618
201643
Time (weeks)